Limnol. Oceanogr., 45(8), 2000, 1764–1772
© 2000, by the American Society of Limnology and Oceanography, Inc.

The response of Chesapeake Bay salinity to climate-induced changes in streamflow

Jody R. Gibson
Environmental Resources Research Institute, Pennsylvania State University, University Park, Pennsylvania 16802

Raymond G. Najjar
Departments of Meteorology and Geosciences, Pennsylvania State University, University Park, Pennsylvania 16802

Abstract

Autoregressive statistical models of monthly salinity variations in the mainstem of Chesapeake Bay are developed for use in climate change applications. Observations of salinity and Susquehanna River flow from 1984 to 1994 are used to calibrate the models. Up to 93% of the variance in salinity is captured by these models, with the best fits occurring in the middle of the bay, where submonthly fluctuations due to river flow and oceanic currents are damped. Our salinity models use output from a climate-forced hydrological model under a doubling of present-day atmospheric CO_2. This coupling scheme predicts salinity changes between +3.5% and −27.5% near the mouth of the Susquehanna River, to between +0.1% and −0.7% near the ocean. These ranges demonstrate the uncertainty in climate model predictions, although three of the four scenarios used indicate increased Susquehanna River flow and therefore decreased salinity. In the highest flow scenario (a 32% annual increase) our results show that the bay's isohalines may recede by approximately 6.3 km (about 2% of the length of the bay) near the Susquehanna River, to as much as 55 km (about 17% of the length of the bay) near the middle bay. This shift implies that climate change may have consequences for organisms with low-salinity thresholds, including oysters and crabs.

Salinity has a profound impact on the physical, chemical, and biological dynamics of estuaries. The most relevant physical consequence of salinity is its effect on density and therefore circulation and stratification (Johnson et al. 1991). Chemical impacts are numerous since most equilibrium and rate constants are salinity dependent. For example, with increasing salinity, pH increases while organic matter solubility decreases (Cai et al. 1998). Many estuarine fauna, including economically important oysters, crabs, and clams, cannot exist below certain salinity thresholds (Jackson and Jesien 1996). Salinity, then, has an important association with estuarine water quality; a simple illustration of this is the observed correlation between the vertical salinity gradient and oxygen depletion in Virginia estuaries (Kuo and Neilson 1987).

Climate change due to increases in atmospheric CO_2 may affect estuarine salinity in a variety of ways. Sea-level rise will likely cause salinity to increase as seawater encroaches landward. Wind-induced changes in ocean currents may also lead to changes in the salinity distribution. Finally, changes in the climate of estuarine watersheds will change riverine freshwater input (Cayan and Peterson 1993; Justić et al. 1996). In this paper, we examine the latter effect for Chesapeake Bay, the largest and most productive estuary in the United States (Schubel and Pritchard 1986; Harding and Perry 1997). Salinity variations in Chesapeake Bay are, to a large extent, driven by flow variations of the Susquehanna River: this river supplies 62% of the gauged freshwater and is the only river that empties directly into the mainstem of the bay (Schubel and Pritchard 1986). Using a simple water balance model of the Susquehanna River Basin (SRB) and the output of four climate models, Najjar (1999) and Neff et al. (2000) estimated that Susquehanna River flow would change by −4% to +33% for a doubling of atmospheric CO_2 over present-day levels. Here, we develop a simple model of salinity variations in Chesapeake Bay and force it with output from the SRB model to estimate salinity changes for a doubling of atmospheric CO_2.

Model development

Models for predicting salinity in Chesapeake Bay exist, but they are either difficult to implement or do not explicitly account for the possibility of environmental change. The empirical models of Wang et al. (1992) and DeSilets et al. (1992) predict salinity as a function of location and time of year, but none of the inputs is river flow. Hydrodynamic models of the bay that are forced by riverine input have been developed (Johnson et al. 1991), but they are computationally demanding and difficult to analyze. Hydrodynamic models have many variables that are difficult to constrain—wind velocity, air temperature, freshwater flow, open ocean boundary conditions, and turbulence parameterizations just to name a few. For predictive purposes, it is desirable to strike a balance between the number of environmental inputs in a model and its ease of implementation.

Here, we adopt statistical methods for modeling salinity in Chesapeake Bay, incorporating flow as the environmental input parameter. Although statistical models have limited use in highly evolving systems, they do have the advantage of simplicity, and accuracy increases with larger data sets. Actually, in the most dynamical of systems, discrete formulations—including regressions—can be more accurate than

Acknowledgments

We would like to thank the United States Environmental Protection Agency for supporting this research under the Johns Hopkins University health grant. Thanks also to Ricky Bahner for providing us with historical salinity data, and to Shuang-Ye Wu for assistance with the map data. Finally, we would like to thank Lee Kump and Rudy Slingerland for preliminary critiques of this manuscript.

smooth analytical models (Roush et al. 1994). Since Chesapeake Bay is a highly variable system (Schubel and Pritchard 1986), it seems appropriate to model its salinity statistically, especially since Chesapeake Bay and the rivers flowing into it have been extensively monitored.

We chose autoregression—the regression of a variable on itself—to model salinity. Modeling salinity autoregressively makes sense on physical grounds because the finite-difference form of the salinity advection/diffusion equation has terms representing past and present values. Additionally, our autoregression scheme incorporates river flow, which resembles the velocity term in a finite-difference scheme for advection. Thus, our basic salinity model is

$$S_t = \alpha_1 S_{t-1} + \alpha_2 S_{t-2} + \cdots + \alpha_n S_{t-n} + \beta_0 F_t + \beta_1 F_{t-1} + \beta_2 F_{t-2} + \cdots + \beta_m F_{t-m} + k, \quad (1)$$

where S_t is the present monthly mean salinity at any particular location and F_t is the present monthly mean flow from the Susquehanna River. S_t, then, is a function of the previous n monthly salinities (S_{t-1} through S_{t-n}), the present month's flow, and the previous m monthly flows. Including several flow lags ensures representation of the month of highest influence, since a packet of freshwater reaches different locations at different times.

Given the form of (Eq. 1), we have the option of running the salinity model with the aid of observed values. This is, in fact, the standard procedure for calculating the skill of a statistical model in reconstructing the calibrating time series. Essentially, what this means is that the output at each time step is *not* fed back into the model—i.e., the model is not actually recursive. This procedure provides a measure of the maximum skill at simulating a time series. In this study, we use three verbs to describe the creation of salinity time series: reconstruct, which applies to both the nonrecursive *and* recursive forms of (Eq. 1); simulate, which only applies to the recursive form of (Eq. 1); and project, which also only applies to the recursive form of (Eq. 1). Evaluation of the model can involve both reconstruction and simulation, but application of the model only involves simulation and projection (the latter referring to the simulation of future values). The reason for this is that there are usually scarce or completely missing data when we want to apply the model; recursive modeling is then necessary, even if our sole interest is to reconstruct such scarce data.

A comprehensive autoregressive Matlab freeware package off of the Worldwide Web (LeSage, www.spatial-econometrics.com) made possible the computation of model coefficients, the r^2 parameter, the t-statistic for the independent variables, and their P values, or significance. The coefficients in (Eq. 1) result from least-squares analysis, and the number of relevant salinity terms, n, derives from the application of Akaike's Information Criterion (AIC). The AIC is a mathematical minimum of the training error and the number of terms being fit; on a plot of serial salinity correlation (autocorrelation) versus lag number, the AIC can be thought of as a horizontal line intersecting the plotted curve at a lag number, n, where the curve's slope becomes small (S-Plus 2000). Autoregressive techniques also allow for the expansion of k into a series of errors in order to further reduce the model residuals to white noise. In this case, the model is classified as a full autoregressive-moving average (ARMA) model (Shumway 1988). In this study, however, not only was there little need for the moving average component in reconstructing the observed, but such a component would have been difficult to constrain for salinity projections. Thus, k here is simply an overall error, or, the model y-intercept.

Dividing the bay into grid cells was necessary to provide a modest two-dimensional resolution of salinity. Therefore, we used the horizontal discretization of Harding and Perry (1997), which is based on the bay's natural salinity zonation, along with four vertical divisions, to produce a total of 24 grid cells. Figure 1 depicts the horizontal and vertical divisions used in this study; they capture the two primary salinity gradient directions in the mainstem bay—north–south and vertical. The vertical divisions are 0–5 m, 5–10 m, 10–15 m, and 15+ m in depth. The numbering convention we adopt is (i, j), where i represents the ith horizontal grid cell starting from the north, and j represents the jth vertical grid cell starting from the surface. Only one cell, numbered (1, 4), lacks a model because the water is too shallow, but each of the remaining 23 cells contains a uniquely different autoregressive model.

Every model contains seven flow terms, although most cells are insensitive to 6-month-old flow. There were several reasons to be more generous and less particular with flow than with salinity inputs. One is that 6 months span the amount of time required to characterize the shape of the mean annual (flow) cycle. Consequently, the applied model should contain enough information at any given time and locale to adequately track seasonal variations. Second, although analyzing each flow term for relevance would provide information on the natural circulation in the bay, there are better ways to achieve this. Such information is not wholly pertinent to this study, as our intent is to model certain effects of climate change through quick and relatively effective means, and using autoregression at all is a statement about the need to study more closely the predicted variable—in this case, salinity. Here, the number of salinity terms, or the order, varies from cell to cell and represents the salinity memory in each cell; this provides a backdrop on which we can analyze our results. Finally, the record of Susquehanna River flow is older and more continuous than salinity data. This simply means that there is no actual limit to the number of flow terms we can include because initializing them is never a problem.

The salinity data in this study, of which only mainstem bay monitoring stations contribute (Fig. 1), were collected by the Chesapeake Bay Water Quality Monitoring Program. Salinity was measured during every month in the period 1984–1994, although the summer months usually contain a greater abundance of observations. There are typically 200 observations per cell per year, taken from about 45 d throughout the year, and we computed monthly averages for each of the 23 cells from 1984 to 1994. Our models are calibrated on observations starting in 1984: in older salinity records, the reduced data density leads to discontinuities in resulting monthly time series. However, despite their patchiness, older records can provide an evaluation for our mod-

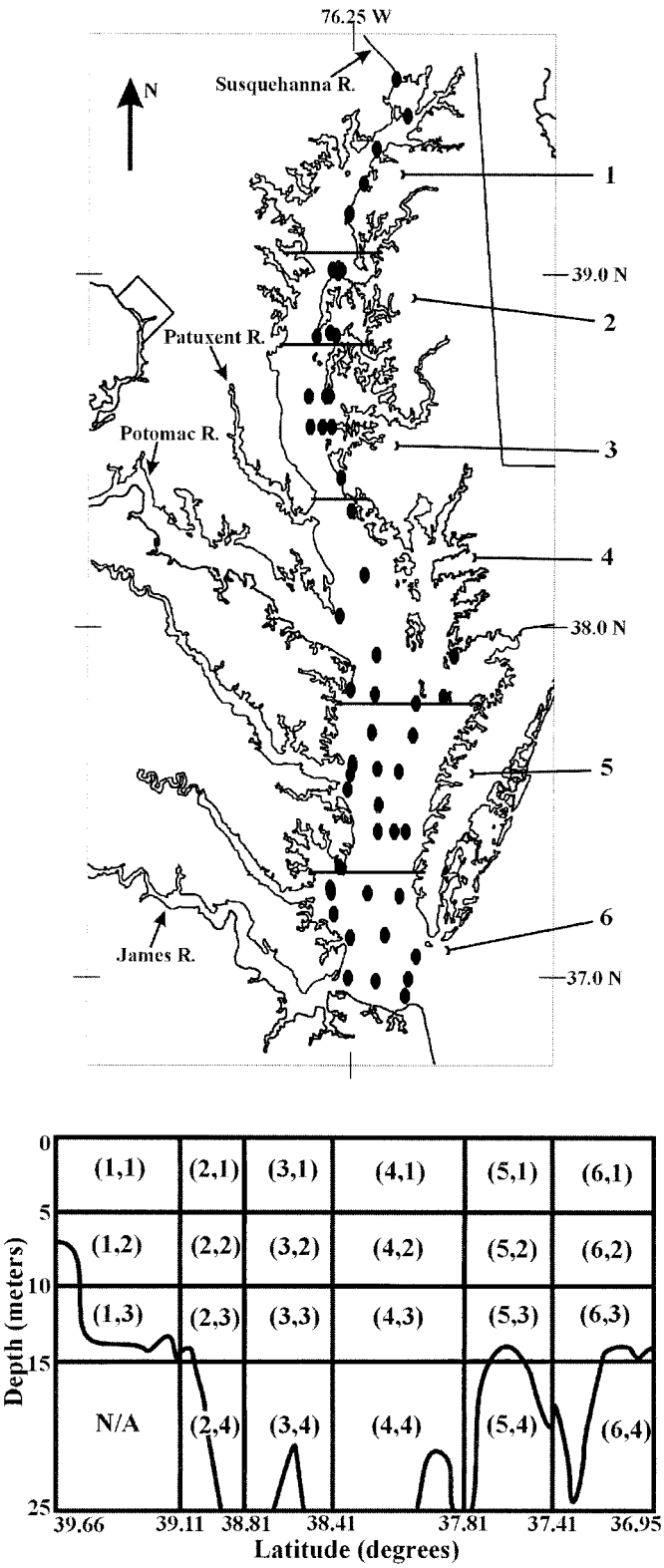

Fig. 1. View of the longitudinal divisions used in this study. Divisions 1 and 2 are the oligohaline region, 3 and 4 are the mesohaline, and 5 and 6 are the polyhaline (after Harding and Perry 1997). Monitoring stations are designated by ovals. Also shown is a relative size grid of the 23 cells created for autoregression. The bottom row (x, 4) contains cells of varying height, as apparent from longitudinal bathymetry (dark line) and the shallowness at (1, 4).

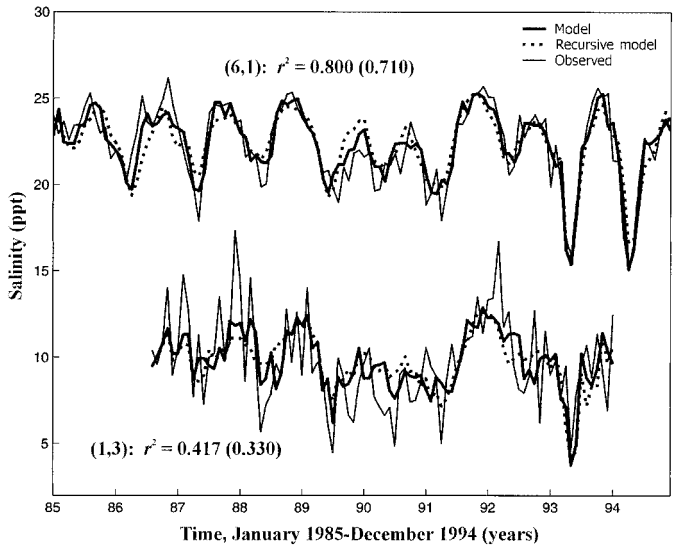

Fig. 2. Time series for the observed and reconstructed salinity in cells (1, 3) and (6, 1) from 1985 to 1994. The r^2 values in parentheses are for the recursive models.

els, so we obtained historical data for 1949–1982 from the Chesapeake Bay Program office archives and computed monthly averages for each cell when possible. The flow data are from the United States Geological Survey (USGS), with daily flow from Harrisburg, Pennsylvania (USGS station number 01570500) and Conowingo, Maryland (USGS station number 01578310); Harrisburg is approximately 100 km upstream of Conowingo Dam, which is about 15 km upstream of the mouth. Monthly averaged flows for Conowingo during 1984–1994 and Harrisburg during 1949–1982 were used. We multiplied the Harrisburg flow by 1.145 (Najjar 1999) to approximate the Conowingo flow during 1949–1982.

Model evaluation

Figure 2 shows reconstructed time series for two of the 23 cells—cell (6, 1), which is at the surface near the bay mouth, and cell (1, 3), which is at the bottom near the Susquehanna River mouth. The model for cell (6, 1) has an r^2 of 0.800, and the model for cell (1, 3) has an r^2 of 0.417. Also shown are the reconstructions from the recursive form of (Eq. 1), and in each cell the skill drops by only approximately 9 percentage points. This fact suggests that autoregressive models such as these are suitable for future projections: despite a lack of stabilizing observations, the recursive reconstructions do not appear to diverge from the observed through time. This point is later discussed in more detail. Time series for cells (1, 3) and (6, 1) together illustrate the importance of the order, n, of a model, which generally increases as variability decreases. The model for (1, 3) is of order 5; the model for (6, 1) is of order 7; and it is clear that the former time series is more variable. One might think that adding terms necessarily improves the model, but the purpose of the autocorrelation plots is to reveal statistically insignificant terms that should be omitted from a model. This

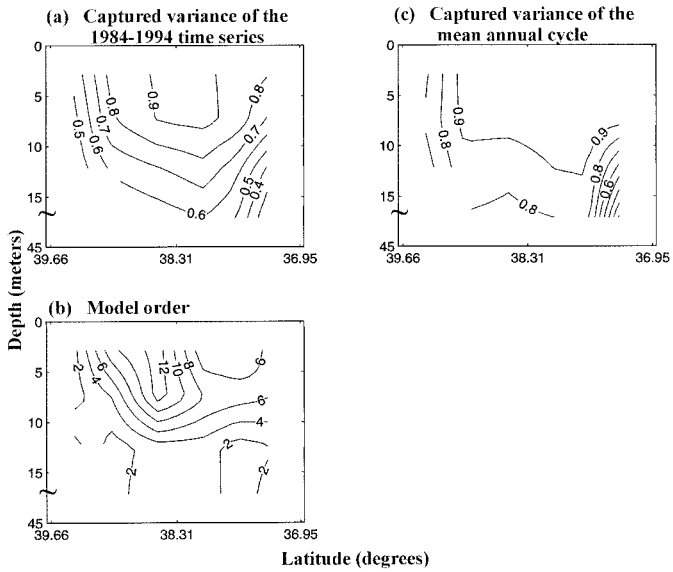

Fig. 3. (a) r^2 values contoured to the various cells in Chesapeake Bay. (b) Contours of model orders. (c) Contours of the r^2 values resulting from reconstruction of the mean annual cycle.

is good for two reasons: it conveys information about memory, as mentioned before, and it makes the models easier to use by minimizing the number of months committed for initialization. Thus, cell (1, 3) has a mediocre model no matter how many terms are included.

Figure 3a shows the distribution of r^2 values resulting from each cell's statistical calibration (values correspond to nonrecursive reconstructions). Notice that regions of poor fit are either near the ocean or the mouth of the Susquehanna River. With the exception of the low skill near the river mouth, the pattern coincides with what we expect from a model forced by flow. Why, though, is the model skill better at midbay than toward the river mouth? Figure 3b, which shows the distribution of salinity lags, provides some insight. Given the fact that the number of salinity lags is approximately inversely proportional to salinity variability, and that Figs. 3a and 3b reveal similar patterns, then we can say that the variability increases from midbay toward the river mouth. Although the reduction in skill toward the bay mouth is most likely due to the framework of our model (i.e., river flow is an inadequate predictor toward the bay mouth), the reduction in skill toward the river mouth is probably a reflection of the difference in sampling rates of salinity and flow. Since salinity in a given cell is sampled much less frequently than flow from the Susquehanna River, it is easy to see how submonthly variations in flow can lead to salinity variations that escape our averaging. Consequently, although salinity and flow are highly correlated near the river mouth, the combination of high variability in flow with infrequent salinity observations leads to an apparently high salinity variability—one that is difficult to model. On the other hand, the high salinity variability at the bay mouth is probably influenced by oceanic factors at least as much as by poor sampling rates. Furthermore, given that salty inflows move along the bottom of the bay, we should expect natural variability to be higher there. We might assume that a whole new modeling approach—perhaps one incorporating tidal salt water flows—is then appropriate (Kuo and Neilson 1987).

Table 1. Summary of the performance of all 23 autoregressive models. Each row corresponds to a separate cell. There are three columns of r^2 values followed by a column providing the model order (number of salinity lags). *See Fig. 1* for the location of each cell.

Cell	r^2*	r^2†	r^2‡	Order
(1, 1)	0.518	0.325	0.667	1
(1, 2)	0.450	0.295	0.707	1
(1, 3)	0.417	0.214	0.639	5
(2, 1)	0.846	0.462	0.941	10
(2, 2)	0.786	0.415	0.928	4
(2, 3)	0.610	0.252	0.864	1
(2, 4)	0.495	0.213	0.785	1
(3, 1)	0.912	0.486	0.965	13
(3, 2)	0.907	0.395	0.942	13
(3, 3)	0.679	0.156	0.822	3
(3, 4)	0.534	0.181	0.770	4
(4, 1)	0.911	0.421	0.972	4
(4, 2)	0.926	0.373	0.968	8
(4, 3)	0.758	0.265	0.900	3
(4, 4)	0.585	0.210	0.793	3
(5, 1)	0.881	0.377	0.954	4
(5, 2)	0.870	0.322	0.960	7
(5, 3)	0.629	0.247	0.907	1
(5, 4)	0.500	0.213	0.854	1
(6, 1)	0.800	0.378	0.943	7
(6, 2)	0.643	0.315	0.932	6
(6, 3)	0.300	0.138	0.455	2
(6, 4)	0.123	0.089	−0.024	3

* The r^2 value resulting from the reconstruction of the calibrating time series (1984–1994).

† The r^2 value resulting from the reconstruction of the calibrating time series using the observed mean annual salinity cycle for that period.

‡ The r^2 value resulting from the reconstruction of the mean annual salinity cycle using the recursive autoregressive model.

Nevertheless, as can be seen in Fig. 3a, a large portion of the bay is above the 0.600 performance range. Even more promising is the model skill shown in Fig. 3c: r^2 values here correspond to an attempt to reconstruct the mean annual cycle in salinity during 1984–1994. We report this skill in order to relate to the form of the model we use for climate change projections. The form of the model in that case is recursive, and its forcing is some mean annual cycle in flow; a point that will be discussed in detail later. In Fig. 3c, the forcing flow is the mean annual cycle during 1984–1994, and the model skill in reconstructing the salinity cycle is much improved over the skill in Fig. 3a. This point is important, because reliability for our climate change projections should hinge more on Fig. 3c than Fig. 3a. Table 1 summarizes the 23 models, including three types of r^2 values and the model orders. The second column of r^2 values is the variance captured by using the observed mean annual salinity cycle as the model; it is apparent that such models typically contribute less than half of the skill accounted for by the autoregressive models. Thus, although our autoregressive models are simple, it is obvious that there is a limit to how simply one can construct an effective salinity model.

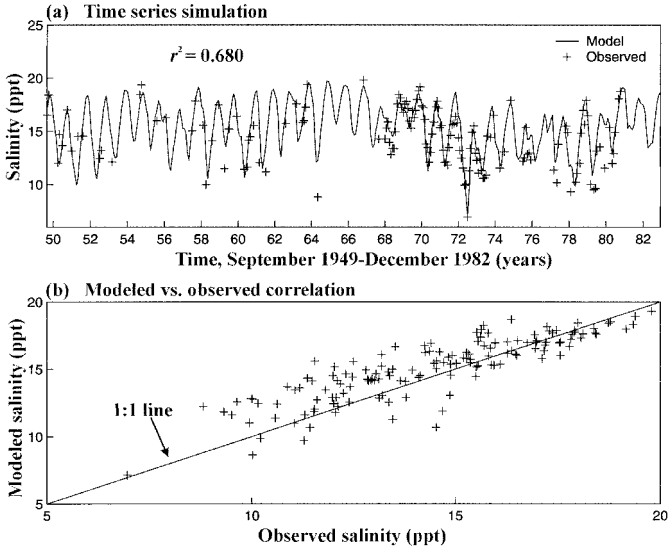

Fig. 4. Historical simulation, 1949–1982, of Chesapeake Bay monthly salinity in (4, 2).

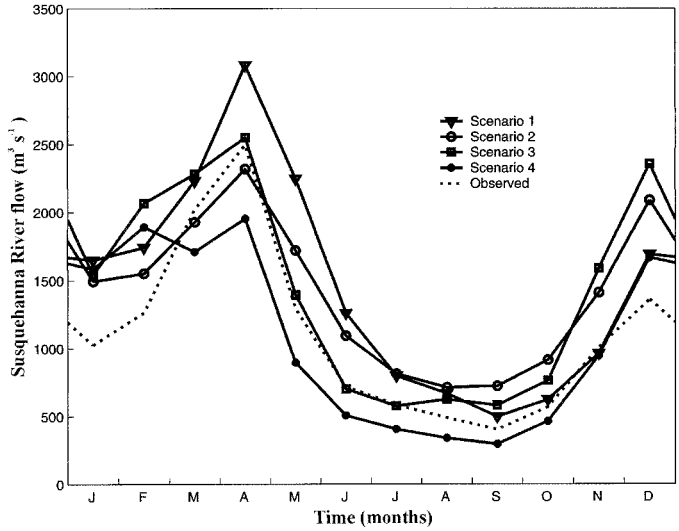

Fig. 5. Flow scenarios used in this study. All values are in cubic meters per second, calculated as monthly averages from daily data. *See text* for descriptions of scenarios.

In order to evaluate the relevance of other Chesapeake Bay tributaries to overall model performance, flow data for the Potomac and James Rivers (Fig. 1) were also analyzed. These two rivers were chosen because they are the second and third largest contributors of freshwater to the bay, respectively. The r^2 distributions resulting from addition of each river's present flow, and its six previous months of flow, were analyzed. Such distributions showed that the Potomac captured up to 10% of the observed salinity variance, whereas the James captured a maximum of another 6%. However, these maximum contributions occurred in different locales, and the optimal improvement was no more than 13% of the observed variance at cell (6, 4). Although this may be significant, the majority of the bay experienced little to no improvement. Furthermore, the cells benefiting most from the additional inputs remain poorly modeled. Finally, a sensitivity analysis—involving flow increases for each river in turn—indicated that the three-river model is physically unrealistic: extra flow from the Potomac actually *increased* salinity in most cells.

Essentially, there are four reasons why flow from the Potomac and James Rivers does not improve the existing models much: (1) the combined flow from those rivers is relatively small compared to that of the Susquehanna River, (2) those rivers do not empty directly into the mainstem bay (Schubel and Pritchard 1986), (3) the rivers are downstream of much of the bay, and (4) a significant portion of monthly mean flow variance in the Potomac (63%) and James (44%) Rivers can be accounted for by the Susquehanna River during 1984–1994.

As noted earlier, the r^2 values in Fig. 3a represent the performance of each model according to (Eq. 1), but using the *observed* salinity values during 1984–1994 as lags. On the other hand, the r^2 values in Fig. 3c reflect the skill that our future salinity projections have. However, to further understand the quality of our autoregressive scheme, testing its performance on data outside of the calibrating time period is important: in this study, we apply the recursive model to discontinuous salinity observations during 1949–1982. Thus, the best model—in this case, the (4, 2) model—was initialized with the modern mean annual salinity cycle and run with observed flow in simulating the historical salinity. The initialization scheme was assumed safe since there was no indication of a trend in the training data. Figure 4 shows the resulting time series against observed values. The fit is promising, with $r^2 = 0.680$, and there is no divergence between the model and the observed. Also, because of the reduced density of salinity observations in the historical record, the monthly time series may exhibit more variability than if the observations had been as frequent as those in the calibrating time period. Therefore, a significant amount of the reduced skill (0.926 to 0.680) may be a result of the data set and not the modeling scheme. Importantly, the model was insensitive to the salinity initialization scheme, which implies that the explanatory variable—river flow here—is quite stabilizing. Thus, we can be relatively sure that our models will avoid any autoregressive artifacts and, instead, respond to prescribed climate change in a physical manner.

Climate change projections

We now briefly describe the four future streamflow scenarios and the means by which they were generated. All of the scenarios (Fig. 5), are based on a coupling of a water balance model of the SRB with the predictions of temperature and precipitation changes from four climate models. The water balance model is spatially averaged over the SRB and has a soil moisture reservoir, a snow reservoir, and a reservoir from which streamflow is generated (essentially groundwater). The model is forced by precipitation and temperature, with the latter being used to estimate rates of evapotranspiration, the partitioning of precipitation into rain and snow, and the snowmelt rate. The model has a handful of parameters that were calibrated to the mean annual cycle

of flow at the mouth of the Susquehanna River ($r^2 = 0.99$). The model is also skillful at simulating monthly variability in flow from 1900 to 1987 ($r^2 = 0.75$). Further details are given in Najjar (1999).

Four separate climate models were used to generate the temperature and precipitation changes used to drive the SRB model. All four scenarios are based on climate model predictions for a doubling of present-day atmospheric CO_2, with the first two being equilibrium responses of atmosphere-only models to an instantaneous doubling of CO_2, and the second two being transient responses of fully coupled ocean-atmosphere models to a gradual increase in atmospheric CO_2. Scenario 1 is based on the nesting of a high-resolution model, known as RegCM2 (regional climate model 2), into the GENESIS global general circulation model (GCM). Details of the model run for the present day are given in Jenkins and Barron (1997) and for a doubling of atmospheric CO_2 in Najjar (1999). Scenario 2 precipitation was generated by applying a neural network downscaling technique to GENESIS climate model output (Crane and Hewitson 1998). No downscaled temperatures were generated, so temperature changes from scenario 1 were used for scenario 2. The use of nesting and downscaling generally increases model skill when compared to the use of the raw GCM output, and these examples are no exception (Jenkins and Barron 1997; Crane and Hewitson 1998). Both models simulate annual mean precipitation well, and both have a summer maximum in precipitation, in agreement with the observations, though the nested model tends to predict too much precipitation during this time. The streamflow predictions based on these models are described in Najjar (1999).

Scenarios 3 and 4 are based on climate models from the Hadley Centre for Climate Prediction and Research and the Canadian Climate Centre (CCC). These state-of-the-art global models were chosen mainly because they are being used by the National Assessment of the Potential Consequences of Climate Variability and Change, which was initiated by the United States Federal Government in 1997. The use of these models in this study facilitates integration with other climate assessment activities. A description of the model results for the mid-Atlantic region of the United States is given in Polsky et al. (2000), and detailed descriptions of the models themselves can be found in references therein. Their skill in reproducing northern midlatitude climate (comparable to SRB climate) is good: they slightly overestimate winter precipitation, but compared to other major GCMs they estimate temperature quite well (Houghton et al. 1996). Results of the climate models from 2090–2099 were used, corresponding to a doubling of atmospheric CO_2 in the models. The streamflow predictions based on these models are described in Neff et al. (2000).

For three of the four models—scenarios 1, 2, and 3—the predictions of annual mean flow change are similar, with increases of 32%, 27%, and 29%, respectively, from the modern mean (1984–1994) flow. The CCC model predicts a much larger temperature increase and a much smaller precipitation increase, which results in a modest (4%) decrease in annual mean flow. Most of this decrease occurs during spring and summer. All four models predict increases in fall and winter flow due to warming-induced snowmelt. The timing of the streamflow increases in the three wettest models, which generally reflects the timing of the precipitation increases: winter and spring for scenario 1, spring and summer for scenario 2, and summer and fall for scenario 3 (Fig. 5).

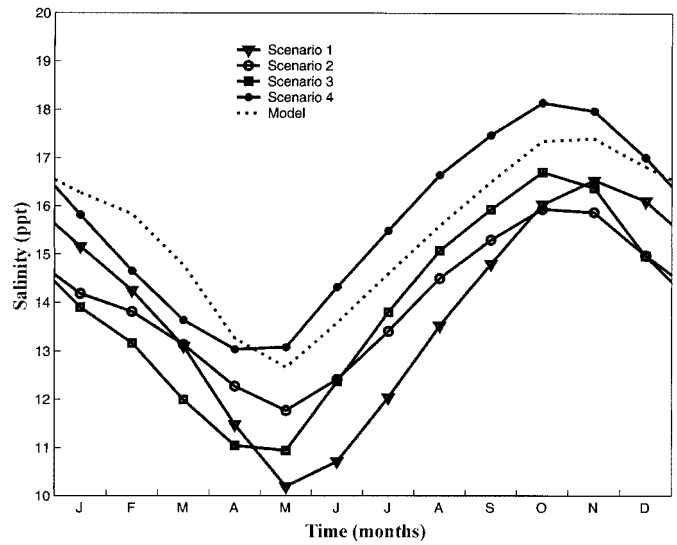

Fig. 6. Mean annual salinity cycles projected for (4, 2) in response to climate change scenarios 1, 2, 3, and 4.

The method we use for projecting climate change impacts is through the simulation of mean annual cycles. The models are initialized with present-day mean annual cycles in salinity and flow; projections are then made by forcing the models with the repeating annual cycle in the predicted streamflow. All salinity projections represent the mean annual cycles of the resulting steady state time series. Figure 6 depicts the climate change impacts on cell (4, 2) for all four scenarios, in addition to the modeled present-day mean annual cycle. The latter is quite skillful, capturing approximately 97% of the variance in the observed cycle (Table 1), which is therefore omitted from the figure for simplification. In reference to the observed/modeled cycle, notice that the amplitude and phasing of the climate change projections differ modestly from the present day. Not surprisingly, the shape of the forcing flow cycles seems to dictate these distortions (Fig. 5): scenario 1 tends to shift the cycle later, scenario 2 tends to force longer winter reductions in salinity, scenario 3 tends to shift the cycle earlier, and scenario 4 tends to force longer summer increases in salinity. The lag of the cycle in scenario 1 is due to the extension of high spring flow through June, whereas scenario 3 cycles earlier because of a large early winter flow peak (Fig. 5). On the other hand, scenario 2 is associated with high flow under normally low flow months, and scenario 4 is associated with low flow under normally high flow months (Fig. 5). Climate change results for other cells are similar to what is seen for cell (4, 2).

The results for the entire bay are shown in Fig. 7, where percent changes in salinity are calculated using the unperturbed model as the reference. This removes the effect of poor model performance when calculating annual mean changes. The parts per thousand (ppt) changes (Fig. 8) are

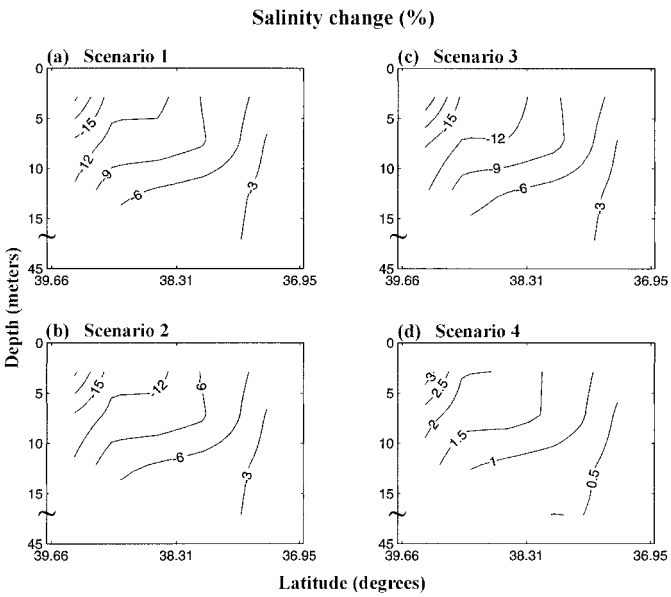

Fig. 7. Climate change impact on Chesapeake Bay for (a) scenario 1, (b) scenario 2, (c) scenario 3, and (d) scenario 4. The contours are isolines of salinity change, in percent deviation from the projected normal means.

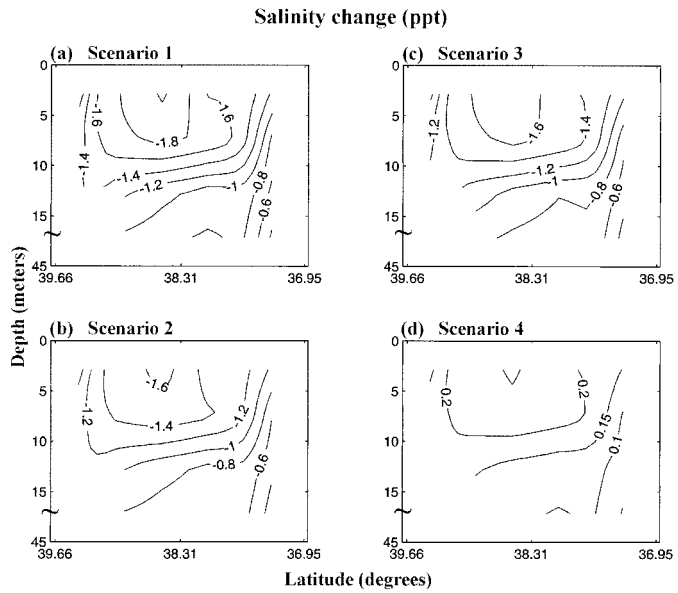

Fig. 8. Climate change impact on Chesapeake Bay for (a) scenario 1, (b) scenario 2, (c) scenario 3, and (d) scenario 4. The contours are isolines of salinity change, in parts per thousand (ppt).

calculated with these percent changes on modern mean salinities to convey a sense of absolute change. Notice that the overall salinity changes directly reflect the respective magnitudes of flow change. Also notice the similarity in spatial distributions of salinity change in all four scenarios: Fig. 7 shows that annual mean salinity control by the Susquehanna River is essentially limited by distance. On the other hand, Fig. 8 shows that large salt *concentration* changes occur in the surface middle bay. This makes sense because the concentration is calculated as a function of the percent changes and the mean background salinity: wherever both of these are substantial is where the ppt changes are greatest. The region of large ppt changes coincides with the region of high memory (Fig. 3), and this supports the idea that fresh and salt water signals add constructively there.

Discussion and conclusions

The results presented here indicate several important characteristics of salinity variation in Chesapeake Bay. Simple statistical models are efficient at capturing the majority of seasonal and interannual variance in much of the bay. The variance that is difficult to capture is probably a result of submonthly fluctuations of the Susquehanna River and continental shelf currents. It might also be possible to improve simulation of the bay's northern and southern extremes by including a tidal flow model component, but this is a nontrivial exercise. In terms of projecting the impacts of future climate change, tidal inputs are probably irrelevant, as tidal flows are unlikely to change, barring massive sea-level rise. Our simple models predict changes in salinity that are consistent with expectations. Although each scenario has its minor distinctions, the resulting salinity cycles are purely functions of location in the bay and the shape of the forcing flow cycle. The first three scenarios agree that salinity in the bay will decrease, anywhere from 22.6% to 27.5% near the mouth of the Susquehanna, to 0.6% to 0.8% near the mouth of the bay. The CCC scenario results in increased salinity—anywhere from 3.5% to 0.1%, depending on distance from the Susquehanna River. In all four scenarios, there is a nearly identical spatial pattern relating annual mean percent flow change to annual mean percent salinity change (Fig. 9), making salinity response predictions straightforward for any scenario.

In order to improve predictions of the response of estuarine salinity to climate change, other factors need to be considered, the most important of which is sea-level rise. Existing approaches for simulating the impact of sea-level rise on salinity are only recently complex enough to handle even two-dimensional dynamics (Kuo 1992). The most widespread models are zero- or one-dimensional models for estuaries with very simple bathymetry (Hull and Titus 1986; Savenije 1986). Although an order of magnitude estimate of the response may be gleaned from these models, they are inappropriate for estimating the spatial and temporal response of salinity in estuaries with complex topography, such as Chesapeake Bay (Fig. 1). We think it likely that a three-dimensional hydrodynamic model will be necessary to simulate the response of Chesapeake Bay salinity to sea-level rise.

In terms of the bay's ecology, this study provides some useful information. Figure 8 suggests that increased flow will increase stratification in the water column, but that reduced flow will reduce stratification. As stratification is significant for the transport of dissolved oxygen, fisheries should be cautious of higher flow and the resulting bottom water hypoxia/anoxia. For shellfish, salinity itself is important, and low-salinity regions seem most at risk. This is because of their particular susceptibility to changes in streamflow, as

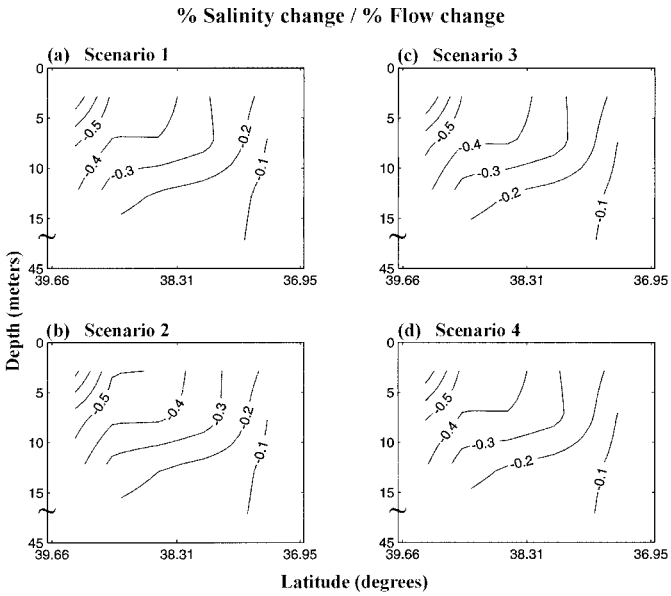

Fig. 9. Relationship between Susquehanna River flow change and Chesapeake Bay salinity change for (a) scenario 1, (b) scenario 2, (c) scenario 3, and (d) scenario 4. Numbers represent the annual mean percent salinity change normalized by the annual mean percent flow change.

well as the fact that the most probable scenario is one involving reduced salinity. Thus, organisms with low-salinity thresholds may exhibit the most change. In particular, the American oyster (*Crassostrea virginica*), which is tolerant of salinities between 5‰ and 30+‰, may see serious declines, as it is already fraught with disease (USEPA 1998). Additionally, the soft shell clam has a low tolerance limit of 8‰, the hard shell clam has high mortality under 12‰, and the blue crab (*Callinectes sapidus*) cannot survive under 20‰ (Jackson and Jesien 1996). Although these organisms are used to naturally large variations in salinity, our results reveal shifts from the mean natural regime. Even without considering the potential for increased salinity variability (for which all but scenario 2 indicate), these salinity shifts imply spatial shifts of habitation zones

Our high flow results yielded sample estimates for maximal isohaline (salt wedge) displacement. These estimates are based on observed salinity gradients at cells (1, 1)/(2, 1) and (3, 1)/(4, 1), respectively. We applied projected salinity changes—the ppt changes at (1, 1) and (3, 1)—to those gradients, yielding distance measures; we then derived percent measures using 320 km for the length of the bay (Schubel and Pritchard 1986). Results show that the salt wedge may recede by from 6.3 km (about 2% of the length of the bay) near the Susquehanna River to as much as 55 km (about 17% of the length of the bay) near the middle bay. This suggests that habitable regions may shrink. Furthermore, decreased salinity can affect the survival rate of virulent bacteria such as cholera; the complex interactions between salinity, cholera, and plankton are difficult to predict, though, since cholera can easily become dormant in planktonic hosts during periods of low salinity (Singleton et al. 1982*a;* Tamplin et al. 1990). Cholera also requires organic matter nutrition (Singleton et al. 1982*b*), and if decreasing salinity increases dissolved organic carbon (DOC), then the bacteria might survive quite well in the surface waters (Cai et al. 1998), where plankton and heat would also be plentiful.

From these speculations, it is even more obvious that further research is needed. As a first attempt at modeling Chesapeake Bay salinity, our simple approach is adequate in some regions, but deficient in others. The utility of this modeling approach, however, is extensive because of its simplicity (it requires only two input variables). Thus, applying it to other estuaries is straightforward as long as there are extensive data. This exercise would be meaningful in the sense that all estuaries may be affected by climate change, particularly through river runoff changes (Miller and Russell 1992). Likewise, the modeling scheme developed here is easily adaptable for reverse calculations, such as reconstructing ancient watershed hydrology and climate using fossil proxies as salinity inputs (Cronin et al. 2000).

References

CAI, W., Y. WANG, AND R. E. HODSON. 1998. Acid-base properties of dissolved organic matter in the estuarine waters of Georgia, USA. Geochim. Cosmochim. Acta **62:** 473–483.

CAYAN, D. R., AND D. H. PETERSON. 1993. Spring climate and salinity in the San Francisco Bay estuary. Water Resour. Res. **29:** 293–303.

CRANE, R. G., AND B. C. HEWITSON. 1998. Doubled CO_2 precipitation changes for the Susquehanna Basin: Downscaling from the genesis general circulation model. Int. J. Climatol. **18:** 65–76.

CRONIN, T., AND OTHERS. 2000. Climatic variability in the eastern United States over the past millennium from Chesapeake Bay sediments. Geology **28:** 3–6.

DESILETS, L., B. GOLDEN, Q. WANG, AND R. KUMAR. 1992. Predicting salinity in the Chesapeake Bay using backpropagation. Comput. Operat. Res. **19:** 277–285.

HARDING, L. W., JR., AND E. S. PERRY. 1997. Long-term increase of phytoplankton biomass in Chesapeake Bay, 1950–1994. Mar. Ecol. Prog. Ser. **157:** 39–52.

HOUGHTON, J. T., L. G. MEIRA FILHO, B. A. CALLANDER, N. HARRIS, A. KATTENBERG, AND K. MASKELL. 1996. Climate change 1995: The science of climate change. Cambridge Univ. Press.

HULL, C. H. J., AND J. G. TITUS. 1986. Greenhouse effect, sea-level rise, and salinity in the Delaware Estuary. U. S. Environmental Protection Agency 230-05-86-010, U.S. EPA and the Delaware River Basin Commission.

JACKSON, D. R., AND R. JESIEN. 1996. Chesapeake Bay low flow study. Susquehanna River Basin Commission.

JENKINS, G. S., AND E. J. BARRON. 1997. Global climate model and coupled regional climate model simulations over the eastern United States: GENESIS and RegCM2 simulations. Glob. Planet. Chang. **15:** 3–32.

JOHNSON, B. H., K. W. KIM, R. E. HEATH, B. B. HSIEH, AND H. L. BUTLER. 1991. Development and verification of a three-dimensional numerical hydrodynamic, salinity and temperature model of Chesapeake Bay. Technical Report HL-91-7, U.S. Army Engineer Waterways Experiment Station.

JUSTIĆ, D., N. N. RABALAIS, AND R. E. TURNER. 1996. Effects of climate change on hypoxia in coastal waters: A doubled CO_2 scenario for the northern Gulf of Mexico. Limnol. Oceanogr. **41:** 992–1003.

KUO, A. Y., AND B. J. NEILSON. 1987. Hypoxia and salinity in Virginia estuaries. Estuaries **10:** 277–283.

KUO, C. Y. 1992. Control of salinity intrusion cause by sea level rise. Environmental Resources Research Institute Technical Report BCS 91-96223, Pennsylvania State Univ.

MILLER, J. R., AND G. L. RUSSELL. 1992. The impact of global warming on river runoff. J. Geophys. Res. **97:** 2757–2764.

NAJJAR, R. G. 1999. The water balance of the Susquehanna River Basin and its response to climate change. J. Hydrol. **219:** 7–19.

NEFF, R., H. CHANG, C. G. KNIGHT, R. G. NAJJAR, B. YARNAL, AND H. A. WALKER. 2000. Impact of climate variation and change on the Mid-Atlantic region hydrology and water resources. Clim. Res. **14:** 207–218.

POLSKY, C., J. ALLARD, N. CURRIT, R. CRANE, AND B. YARNAL. 2000. The Mid-Atlantic Region and its climate: Past, present, and future. Clim. Res. **14:** 161–173.

ROUSH, W. B., G. F. BARBATO, AND T. L. CRAVENER. 1994. A nonlinear dynamical (chaos) approach to the analysis of broiler growth. Poultry Sci. **73:** 1183–1195.

SAVENIJE, H. H. G. 1986. A one-dimensional model for salinity intrusion in alluvial estuaries. J. Hydrol. **85:** 87–109.

SCHUBEL, J. R., AND D. W. PRITCHARD. 1986. Responses of upper Chesapeake Bay to variation in discharge of the Susquehanna River. Estuaries **9:** 236–249.

SHUMWAY, R. H. 1988. Applied statistical time series analysis. Prentice Hall.

SINGLETON, F. L., R. ATTWELL, S. JANGI, AND R. R. COLWELL. 1982*a*. Effects of temperature and salinity on *Vibrio cholerae* growth. Appl. Environ. Microbiol. **44:** 1047–1058.

———, ———, ———, AND ———. 1982*b*. Influence of salinity and organic nutrient concentration on survival and growth of *Vibrio cholerae* in aquatic microcosms. Appl. Environ. Microbiol. **43:** 1080–1085.

S-PLUS. 2000. Guide to statistics, vol. 2. Data Analysis Products Division, MathSoft.

TAMPLIN, M. L., A. L. GAUZENS, A. HUQ, D. A. SACK, AND R. R. COLWELL. 1990. Attachment of *Vibrio Cholerae* serogroup O1 to zooplankton and phytoplankton of Bangladesh waters. Appl. Environ. Microbiol. **56:** 1977–1980.

U.S. ENVIRONMENTAL PROTECTION AGENCY. 1998. Condition of the Mid-Atlantic estuaries. 600-R-98-147, U.S. EPA.

WANG, Q., B. L. GOLDEN, E. A. WASIL, AND G. DINARDO. 1992. Modeling salinity dynamics in the Chesapeake Bay. Am. J. Math. Manag. Sci. **12:** 227–245.

Received: 22 April 2000
Accepted: 18 July 2000
Amended: 24 August 2000